

# 1D LINEAR INTENSITY SPIKING EVOLUTION IN A SINGLE SHOT OF A SASE FEL

C. Maroli, L. Serafini, INFN-Sezione di Milano, Via Celoria 16, 20133 Milano, Italy  
 V. Petrillo, Dipartimento di Fisica dell'Università di Milano-INFN Sezione di Milano,  
 Via Celoria 16, 20133 Milano, Italy

## Abstract

It is shown that the simple system of equations used by Bonifacio et al. in 1994, leads to signals characterized by the usual spiky behaviour of the FEL radiation intensity, as well as to “coherent” signals in which the spiking is reduced to a small amplitude random fluctuation on a smooth and nearly constant average value. The two types of signals are obtained with different classes of initial conditions. In particular, coherent signals correspond to initial shot-noise configurations whose closely spaced spikes have widths much smaller than the cooperation length.

## INTRODUCTION

The intensity spiking in the radiation of a high-gain free-electron laser starting from noise consists of a sequence of random spikes with wide top-to-bottom variations in the signal received at the end of the undulator [1-4]. The random nature of the spiking is a direct consequence of the random character of the small electromagnetic fields created on the electron beam as it enters the undulator field and the main aspects of the spiking are described accurately by the linear form of the one-dimensional FEL equations.

Starting from the Maxwell-Lorentz 1D equations, the disturbances in the radiation field  $\delta A(z,t)$  and bunching factor  $\delta b(z,t)$  are given by the following simple linear system in the limit of small radiation fields and when the radiation wave length  $\lambda$  is much smaller than the cooperation length  $L_C = \lambda/4\pi\rho$  ( $\rho$  is the FEL parameter):

$$\left(\frac{\partial}{\partial t} + c(1 - \beta_0)\frac{\partial}{\partial z}\right)\delta A(z,t) = \delta b(z,t),$$

$$\frac{\partial^2}{\partial t^2}\delta b(z,t) = \frac{i}{T_G^3}\delta A(z,t) \quad (1)$$

These equations are written in the frame moving with the undisturbed beam velocity  $c\beta_0$ ,  $T_G = \lambda_w/4\pi c\rho$  is the gain time and  $\lambda_w$  the undulator period. The reason why we reconsider this very simple system of equations is that it may lead to final situations in which there is no spiking and the signal found at the end of 10-20 gain times  $T_G$  consists of one single and smooth bump, even when the length  $L_b$  of the beam is much longer than the cooperation length  $L_C$ .

## ONE SINGLE SPIKE

We consider the particular solution of (1)

$$\delta A(\bar{z}, \bar{t}) = \int_{-\infty}^{+\infty} dh \delta A_0(h) e^{i(h\bar{z} - \alpha(h)\bar{t})}$$

where  $\alpha(h)$  is the root of the dispersion relation  $\omega^3 - h\omega^2 - 1 = 0$  with positive imaginary part. The integral in the preceding equation is solved numerically for the case of a Gaussian spike at  $t=0$  and different values of the parameter  $\alpha = L_0/L_C$ , where  $L_0$  is the FWHM value of the initial Gaussian spike.

Fig.1 shows that the time evolution of the spike depends on the value of its width at  $t=0$  as compared with  $L_C$ . In particular, when  $L_0 \approx L_C$ , the spike increases exponentially while its width increases only slightly. Instead, when  $L_0 \ll L_C$ , the width of the spike increases by several orders of magnitude starting from the very small value at  $t=0$ .

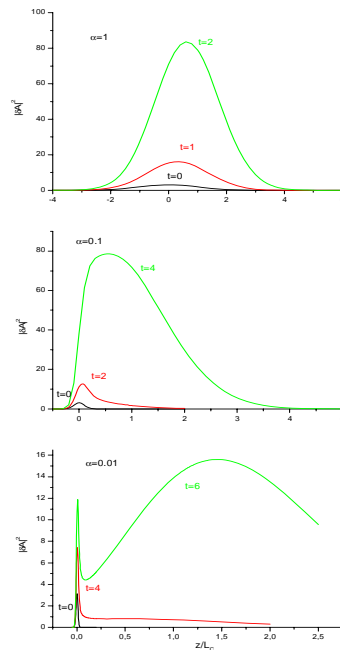


Fig.1(color) – Values of  $|\delta A|^2$  vs  $z/L_C$ . Top figure  $\alpha = 1$ , curves (a, black),(b, red),(c, green) for  $t/T_G = 0, 1, 2$ , respectively; middle figure  $\alpha = 0.1$ , (a),(b),(c) for  $t/T_G=0, 2, 4$ ; bottom figure  $\alpha = 0.01$ , (a),(b),(c) for  $t/T_G=0, 4, 6$ .

Fig.2 shows what happens for large values of  $t/T_G$  and for  $\alpha = 1, 0.1, \text{ and } 0.01$ , while Fig.3 gives the value of the radiation intensity at the peak of the spike vs  $t/T_G$ .

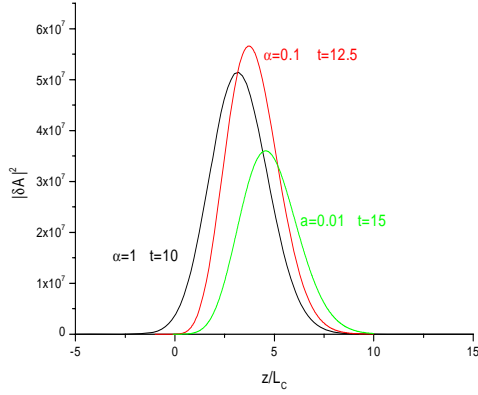


Fig.2 (color) – Values of  $|\delta A|^2$  vs  $z/L_C$ . Curve (a, black)  $\alpha = 1$ ,  $t/T_G = 10$ ; curve (b, red)  $\alpha = 0.1$ ,  $t/T_G = 12.5$ ; curve (c, green)  $\alpha = 0.01$ ,  $t/T_G = 15$ .

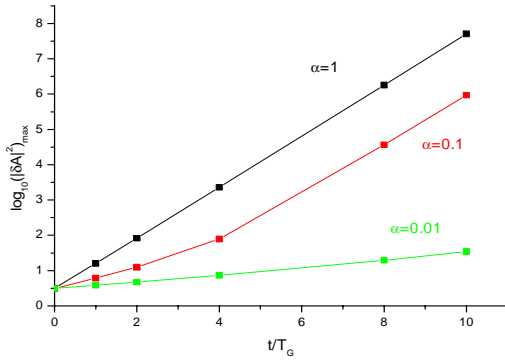


Fig.3 (color) –  $|\delta A|^2$  at the maximum of the spike vs  $t/T_G$  for: (a, black)  $\alpha = 1$ ; (b, red)  $\alpha = 0.1$ ; (c, green)  $\alpha = 0.01$

## RANDOM SEQUENCE OF SPIKES

### *Infinitely long electron beam*

In this case we assume  $\delta A(z,0)$  as the following random sequence of Gaussian spikes

$$\delta A(\bar{z},0) = \sum_{j=1}^{N_{sp}} A_{0j} e^{-\mu_j(\bar{z}-\bar{z}_{0j})^2 + i\theta_j \bar{z}}$$

where  $N_{sp}$  is the number of spikes, the peak of each single spike being at  $z=z_{0j}$  while the complex numbers  $A_{0j}$  and the real numbers  $\mu_j$ ,  $\theta_j$  and  $z_{0j}$  are all random functions of the integer  $j$  defined in terms of their average values and r.m.s. deviations.

Fig.4 shows modulus and phase of the complex number  $\delta A$  at  $t=0$  and  $t=10T_G$  for an initial random sequence in which all spikes have widths comparable with  $L_C$ , the average distance  $D_{sp}$  between successive

spikes being  $5L_C$ . At  $t=10T_G$ ,  $|\delta A|^2$  has the usual spiky form with wide top-to-bottom variations of the signal intensity. Fig.5 shows modulus and phase of  $\delta A$  at  $t=0$  and  $10T_G$ , for a sequence of spikes whose widths are all much smaller than  $L_C$ . In this case the signal at  $t = 10T_G$  has only a small amplitude fluctuation on top of a smooth and nearly constant average value. The number of “spikes” that characterise the shape of the signal intensity at this time follows approximately the usual rule, i.e., number of spikes  $\sim$  bunch length /  $2\pi L_C \sim 40/2\pi \sim 6-7$ , but the amplitude of the spikes as compared with the average value of the intensity is much reduced. The two parts (d) in figures 4 and 5 show the profile of the signal intensity at  $t=10T_G$  for the two cases, together with the corresponding incoherent and interference terms.

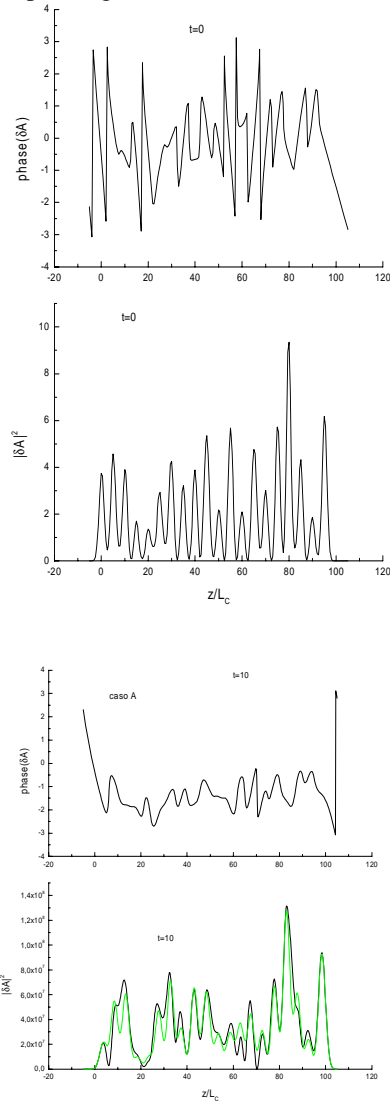


Fig.4 (color) – Phase and modulus squared of  $\delta A$  vs  $z/L_C$  at  $t=0$  (first column, parts (a) and (b)) and  $t=10T_G$  (second column, (c) and (d)). (d) shows the signal intensity (curve 1, black) and the incoherent part (curve 2, green).  $N_{sp}=20$ ,  $D_{sp}=5L_C$ ,  $\alpha=1$ .

While  $|\delta A|^2$  in Fig.4 is practically equal to its incoherent part indicating that the interference between different signals is always negligible, in Fig.5 the final signal intensity is the result of a strong process of constructive interference. If it seems appropriate to classify as “incoherent” the signal produced in the case of Fig.4, it seems likewise appropriate to consider as “coherent” the signal produced in the case of Fig.5.

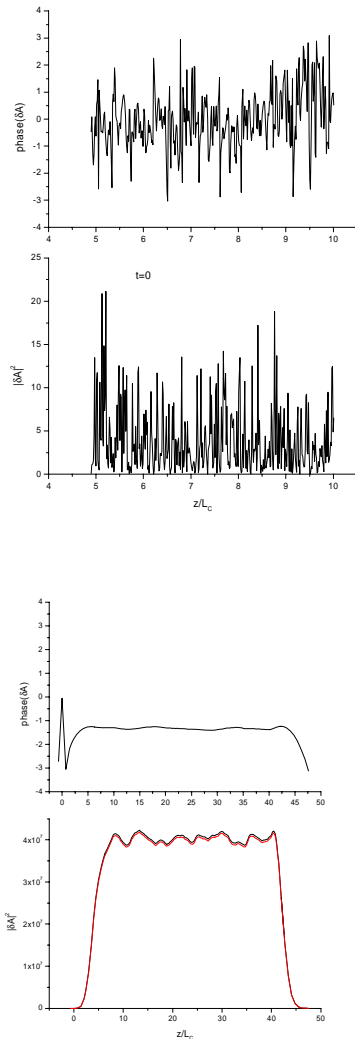


Fig.5 (color) – Same as Fig.6 with  $N_{sp}=1000$ ,  $D_{sp}=0.04$ ,  $L_C$ ,  $\alpha=0.007$ . Only part of the signal has been plotted at  $t=0$ . Part (d) shows the signal intensity (curve 1, black) and the interference part (curve 2, red).

As a third example, we consider the case in which the signal at  $t=0$  contains two characteristic lengths, the first of the order of the cooperation length  $L_C$  and the second much shorter than  $L_C$ . Fig.6 shows what happens in a case in which the initial signal is made up by 225 narrow spikes whose widths are uniformly of the order of  $10^{-1} L_C$  (the average distance between narrow spikes is  $0.2$

$L_C$ ), together with 15 large spikes whose widths are uniformly of the order of  $L_C$  (average distance between large spikes  $3 L_C$ ). The whole signal at  $t=0$  covers about 45 cooperation distances. As one can see, spiking develops also in this case after a considerable “cleaning” of the signal, because at  $t=10 T_G$  it is composed by 8 large spikes (number of spikes  $\sim 45/2\pi \sim 7-8$ ) with the usual wide top-to-bottom oscillations. This is due to the long spikes at  $t=0$  increasing immediately with the largest growth rates.

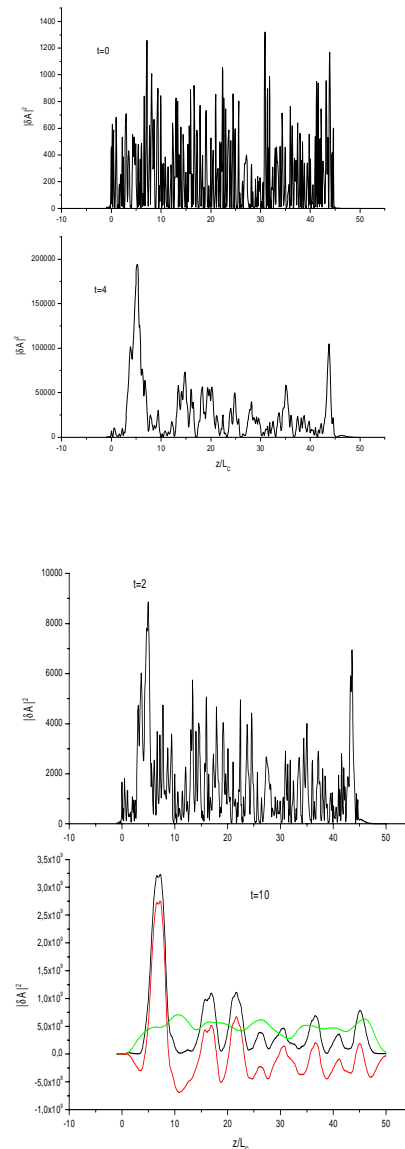


Fig.6 (color) -  $|\delta A|^2$  vs  $z/L_C$  at  $t/T_G=0,2,4,10$  (part (a),(b),(c),(d) respectively). (d) shows also the incoherent (curve 2, green) and interference (curve 3, red) parts of the total signal (curve 1, black) at  $t=10T_G$ .

*Finite-length electron beam*

System (1) has been integrated numerically also in the case of a beam of finite length. Fig.7 shows the behaviour of the signal intensity as obtained by solving the system with appropriate initial and boundary conditions. The initial condition for this case consists of 8000 Gaussian spikes with the average distance between successive spikes  $D_{sp} = 0.01L_C$ . The bunch length is  $L_b = 80 L_C$ .

**CONCLUSION**

The main result of this paper is that according to system (1), the light emitted by an FEL is not always a chaotic light even if the initial signal is noisy [5]. In fact, this system leads to signals dominated by the spiking as well as to signals in which the spiking is reduced to a small amplitude fluctuation superimposed on a smooth pulse. Spiking in the usual sense is associated with initial conditions characterized by a scale-length  $L_0$  of the order of the cooperation length  $L_C$ , while absence of spiking requires that the initial shot-noise condition consists of a random sequence of uniformly narrow spikes with widths of the order of  $10^{-2} L_C$  or smaller, i.e., that  $L_0 \ll L_C$ . Since system (1) is based on the slowly-varying envelope approximation (SVEA), the initial conditions are consistent with its nature only if the characteristic length  $L_0$  is longer than the wave-length  $\lambda$  of the emitted radiation. Absence of spiking as deduced on the basis of (1), therefore, requires that  $L_0$  satisfies the inequality  $\lambda < L_0 \ll L_C$ . This means small values of the FEL parameter  $\rho$ , of the order of  $10^{-4}$  or smaller which are typical of FELs based on static or optical undulators and operating in the regime of very high frequencies or even X-ray FELs.

**REFERENCES**

- [1] R. Bonifacio, L. DeSalvo, P. Pierini, N. Piovella, C. Pellegrini, *Phys. Rev. Letters* **73**, 70 (1994)
- [2] L. H. Yu, S. Krinsky, *Nucl. Instrum. Methods Phys. Res., Sect. A* **407**, 261 (1998)
- [3] E. L. Saldin, E. A. Schneidmiller, M. V. Yurkov, *Opt. Commun.* **148**, 383 (1998)
- [4] K.-Je Kim, in *Towards X-ray Free Electron Lasers*, edited by R. Bonifacio and W. Barletta, AIP Conference Proceedings No. 413 (AIP, New York, 1997), p. 3
- [5] Zhirong Huang, K.-Je Kim, *Phys. Rev. STAB* **10**, 034801 (2007)

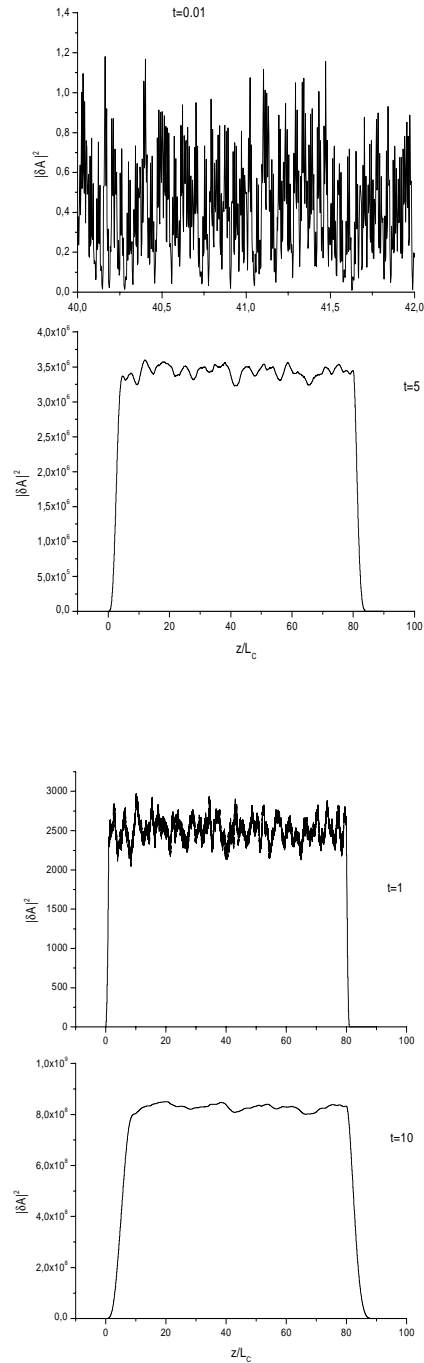


Fig.7 – Signal intensity vs  $z/L_C$  at times  $t/T_G = 0.01, 1, 5, 10$  (parts (a), (b), (c) and (d)) in the case of a finite-length electron beam with  $L_b = 80 L_C$ .  $N_{sp} = 8000$ ,  $D_{sp} = 0.01L_C$ . Only part of the signal is given at  $t=0.01$ .